Physical Science International Journal
4(8): 1050-1064, 2014

SCIENCEDOMAIN *international*
www.sciencedomain.org

Analytical Investigation of Electrons Capture Time Effect on the Threshold Current Density Reduction in QD Spin-Lasers

S. N. Hosseinimotlagh[1*], H. Ghavidelfard[2] and A.Shakeri[3]

[1]Department of Physics, Shiraz branch Islamic Azad University, Shiraz, Iran.
[2]Department of Physics, Payam Noor University, Bandar Abbas, Iran.
[3]Department of Physics, Islamic Azad University, Arsenjan Branch, Fars, Iran.

Authors' contributions

This work was carried out in collaboration between all authors. Author SNH designed the study, performed the statistical analysis, wrote the protocol and wrote the first draft of the manuscript. Authors HG and AS managed the analyses of the study. All authors read and approved the final manuscript.

Original Research Article

Received 22nd February 2014
Accepted 24th April 2014
Published 16th June 2014

ABSTRACT

In this paper, we solve numerically the rate equations governing the $InAs/GaAs$ semiconductor spin with un-polarized and polarized laser field based on quantum dot active region in which $MnAs/Al_{0.1}Ga_{0.9}As$ Schottky tunnel barrier treats as the spin injector. We demonstrate simultaneously the effects of electron capture time, and injected current polarization on threshold current density reduction and normalized spin-filtering interval. The threshold current density reduction and normalized spin-filtering interval increases simultaneously with electrons capture time reduction and increase of injected current polarization. The maximum obtained threshold current density reduction and normalized spin-filtering interval values are0.353 and 0.90, respectively. We also calculate the spin-up optical gain and obtain the conditions for achieving optimum optical gain. The maximum obtained spin-up optical gain value is 17.70.

Keywords: Spin laser, gain; threshold current; quantum dot; filtering.

[*]Corresponding author: Email: hoseinimotlagh@hotmail.com;

1. INTRODUCTION

The importance of lasers generally reflects their practical applications [1-5]. Semiconductor lasers are important due to their widespread applications [3]. Semiconductor lasers use semiconductors as active medium [4]. An active material is pumped to create population inversion and light can be amplified through stimulated emission [3-4]. By the introduction of spin-polarized carriers which is the physical mechanism that enhances stimulated emission [3], the current density threshold in semiconductor lasers can be reduced [6-13]. Such semiconductor lasers are called semiconductor spin polarized-lasers (SSPLs) [14-16]. Most of the SSPLs are vertical cavity surface emitting lasers (VCSELs) with an active region consisting of III–V Quantum Dots (QDs). The VCSELs are types of semiconductor lasers with perpendicular laser beam emission. A VCSEL should have a resonant cavity with two distributed Brag reflectors (DBRs). A DBR is a light reflecting device based on Brag reflections in a periodic structure, alternating high and low refractive indices and with quarter-wave length thick material. It must be highly optically reflective and electrically conductive. An advantage of such laser is low power consumption, low threshold current and generates less heat, but it also has a lower output power than other semiconductor lasers [10-11]. In this paper, we intend to investigate simultaneously the effects of electrons capture time and injected current polarization on threshold current density reduction (TCDR) and normalized spin-filtering interval (NSFI) of a QD SSPL by its numerical rate equation solution. To achieve this aim, we introduce spin polarized injection and present proper materials to implement this (section 2). In section 3 have been represented numerically, the solution of rate equations governing the $InAs/GaAs$ QDs semiconductor spin with un-polarized and polarized laser field by considering quadratic spontaneous radiative recombination [12]. As the creation of NSFI and TCDR are two important consequences of spin polarized injection, we compute the effects of injected electron current polarization and electron capture time on NSFI and TCDR by spotting quadratic spontaneous radiative recombination in section 4 and 5, respectively. In section 6, we calculate spin-up optical gain and obtain the conditions for achieving optimum optical gain. Finally, we present conclusion and discussion in section 7.

2. SUITABLE MATERIALS FOR SPIN-POLARIZED INJECTION

Spin-polarized electron injection into semiconductors has been a field of growing interest during the last years [17]. Since we need electron injection for electronic devices, spintronics devices require spin-polarized electron injection. A spin-polarization of the current is expected from the different conductivities resulting from the different densities of states for spin-up and spin-down electrons in the ferromagnetic materials. A comfortable way of creating spin-polarized electron injection is by passing electron current through ferromagnetic materials. Spin injectors are materials which create spin-polarized electron injection [4]. There have been many choices for spin injectors but the most obvious choice is ferromagnetic materials due to their high Curie temperatures, low coercivities and fast switching times [11-15]. The main problem using ferromagnetic materials is conductivity mismatch, which occurs at the interface between ferromagnetic, and semiconductor materials [18]. There are three solutions for this problem. The first solution is to use half metallic ferromagnetisms [19] which are materials that possess a band-gap at the Fermi level for one of the spin sub-bands, generally the minority-spin sub-band, making them 100% spin-polarized [19]. The second solution is to use diluted magnetic semiconductors, which have similar conductivity with magnetic materials. Note that Curie temperature of these materials is still well below room temperature. Another solution is to use either an

extrinsic or intrinsic tunnel barrier [18]. The advantage of using a tunnel barrier is that it allows ferromagnetic materials to be used as the source of spin-polarized electrons [15]. An intrinsic Schottky barrier is formed when a ferromagnetic material is placed in contact with a semiconductor. It overcomes limitations of the conductivity mismatch without the need for the deposition of a tunnel barrier [15].

3. RATE EQUATIONS

The electronic transitions shown in Fig. 1, take place between conduction and valence band carriers in QD-SSPLs [20].

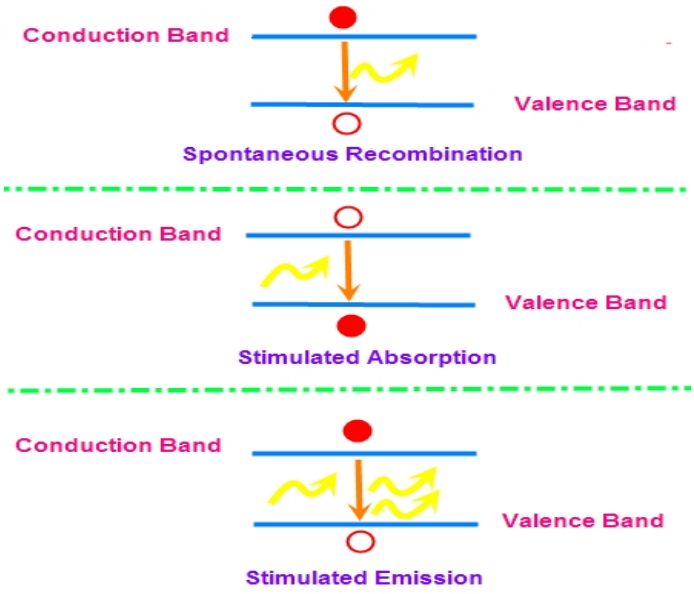

Fig. 1. The electronic transitions in a semiconductor material [20]

The first of the processes is spontaneous recombination of an electron in the conduction band and a hole in the valence band, which results in incoherent emission. The second process is the photon absorption by the active material, which promotes the generation of an electron-hole pair and increases the carrier density in both the conduction band and valence band. The third transition is the emission of a photon by means of an electron-hole recombination after the stimulus of another photon already present in the cavity. This process provides optical gain because it starts with one photon and ends with two photons. The dynamics of carrier and photon densities in semiconductor lasers are governed by the coupled rate equations. The rate equations describe how electrons and holes turn into photons. For simplicity, let us assume a constant current injection rate i.e. at each unit time amount of electron is injected into the laser active region. This pumping process as a photon absorption process in the semiconductor material increases the number of electrons in the conduction band and holes in the valence band while the Photon-emitting processes reduce this number of electrons. The photon-emitting processes are those which generate photons through spontaneous recombination and stimulated emission. Stimulated emitted photons and the spontaneous recombination processes will contribute to increase the photon density, because these processes are producing light inside the device, whereas the photons

involved in the stimulated absorption processes cause the opposite effect, thus decreasing the photon number in a time interval. Beside the stimulated absorption, the material optical loss will also reduce the photon density and expresses how many photons are lost as they propagate at each centimeter of the cavity and as they impinge on the cavity end mirrors.

The QD (Quantum Dot) confine carriers from wetting layer (WL) which acts as a source of carriers. The presence of the WL will affect the dynamical behavior of the device. In QD semiconductor lasers, WL are inevitably present, because of the self-assembly growth process. QD semiconductor lasers will require lower levels of current injection to reach threshold and to keep operating, and the threshold current will be ideally temperature-insensitive. Each electron of the current is directly injected into the WL and become confined in the WL for a given time, after which it will relax into QD. Besides the possibility to relax into QD, an electron in the WL can either spontaneously recombine with a hole of the valence band or undergo a stimulated emission process, generating a photon of energy *"hu"* equal to the energy of the incident photon. The electrons, which get out of the QD don't contribute to the lasing. For the electrons relaxation in QD, the escape from QD implies a confinement in the WL. (see Fig. 2) By assumption of neutrality of charge, rate equation of QD semiconductor lasers in terms of levels occupancy probability by electrons in QDs and WL (f_w, f_{qn}) and photon f_s occupancies is written as [21,22].

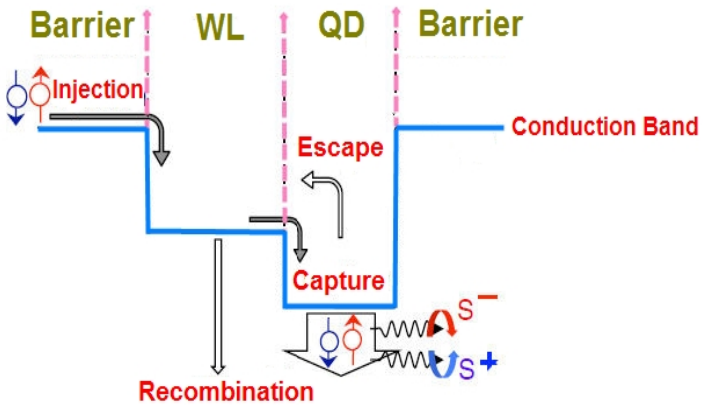

Fig. 2. Characteristic processes in QD SSPL [21]

$$\frac{df_w}{dt} = J(1-f_w) - \frac{f_w(1-f_{qn})}{\tau_c} + \frac{2f_{qn}(1-f_w)}{k\,\tau_e} \tag{1}$$

$$\frac{df_{qn}}{dt} = \frac{kf_w(1-f_{qn})}{2\tau_c} - \frac{f_{qn}(1-f_w)}{\tau_e} - b_q f_{qn}^2 - g(2f_{qn}-1)f_S \tag{2}$$

$$\frac{df_S}{dt} = g(2f_{qn}-1)f_S - \frac{f_S}{\tau_{ph}} \tag{3}$$

where J, τ_c, τ_e, k, b_q, τ_{ph} and g are number of electrons injected into the laser per WL state and unit time, electron capture time, electron escape time, rate of states number in the WL to numbers of QDs, recombination rate in QD, photon lifetime and stimulated emission rate, respectively. Note that spontaneous emission factor and optical confinement factor in equation (3) is 0 and 1, respectively. We neglect spontaneous radiative recombination in equation (1). For the sake of simplicity, we assume a constant current injection rate. This means that at each unit time a very precise amount of electron is injected into the laser active region (this is called the pumping process). The results obtained respectively in equations (1) and (2) are the essential of our investigations (the time dependency of levels occupancies probability by electrons in WL and QDs at fixed injection). Following the numerical representations in Figs. 3 and 4, respectively we find that these results approach the experimental data of reference [22].

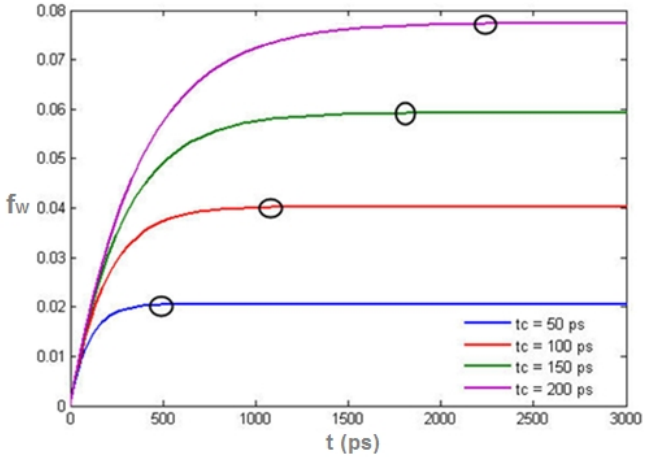

Fig. 3. Time dependency of WL levels occupancies probability by electrons of a QD semiconductor laser

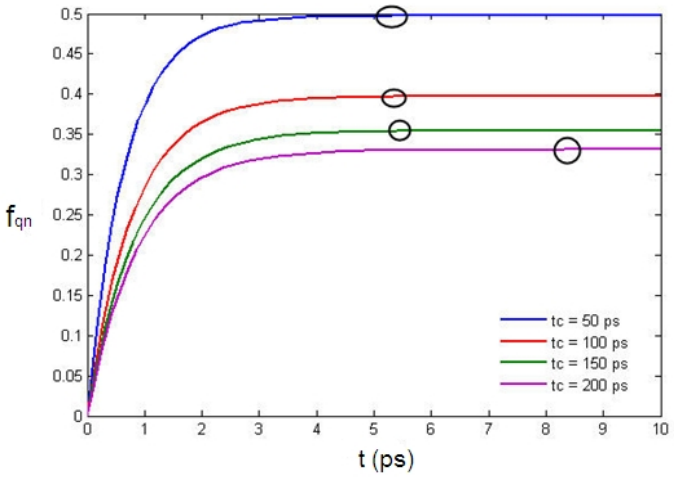

Fig. 4. Time dependency of QD levels occupancies probability by electrons of a QD semiconductor laser

According to these Figs, level occupancy probabilities by electrons in WL increases with increase in electron capture time by electron capture time grow up while level occupancy probabilities by electrons in QD increases with decreases in electron capture time at the fixed injection. As electrons are directly injected to WL, when electrons capture time is shorter, electrons confined in the QDs faster and level occupancy probabilities by electrons increase in QD. As shown in Figs. 3 and 4, from points that are characterized with black circle, level occupancy probability by electrons in QDs and WL have constant trend and saturation is reached. Tables 1 and 2 illustrates obtain values of level occupancy probabilities by electrons in QDs and WL for three various electron capture time.

Table 1. Obtained values of electron occupancies in WL for three various electron capture times

$\tau_c = 50ps$		$\tau_c = 100ps$		$\tau_c = 150ps$	
f_w	$t(ps)$	f_w	$t(ps)$	f_w	$t(ps)$
0.0125	91.7065	0.0207	137.8592	0.0418	344.1086
0.0197	308.7805	0.0389	638.1196	0.0564	850.4725
0.0205	527.0261	0.0402	1155.8	0.0592	1814.9

Table 2. Obtained values of levels occupancy probability by electrons in QDs for three various electron capture times

$\tau_c = 50ps$		$\tau_c = 100ps$		$\tau_c = 150ps$	
f_{qn}	$t(ps)$	f_{qn}	$t(ps)$	f_{qn}	$t(ps)$
0.1346	0.2093	0.1297	0.3139	0.1268	0.3767
0.4928	3.1134	0.3943	3.8449	0.3520	4.1493
0.4972	5.3287	0.3970	5.3449	0.3542	5.6493

Fig. 5 shows time dependency of photon occupancies. According to this Fig, photon occupancies increase by increase of level occupancy probabilities by electrons in QD at the fixed injection. When level occupancy probabilities by electrons increase in QD, the numbers of electrons, which participate in lasing operation increase. Thus, gain increase refers to more coupling of the carriers and light. Therefore, this situation gives rise to stimulated emission and lasing operation is improved.

Table 3 demonstrates obtained values for photon occupancies for three various level occupancy probabilities by electrons in Quantum Dot (QD).

Table 3. Obtained values of photon occupancies for three various levels occupancies probability by electrons in Quantum Dot (QD)

$f_{qn} = o.70$		$f_{qn} = o.73$		$f_{qn} = o.75$	
f_S	$t(ps)$	f_S	$t(ps)$	f_S	$t(ps)$
0.1568	2.2500	0.2377	2.2788	0.3869	2.7059
0.2858	5.2500	0.7433	5.2788	1.5283	5.4534
0.6360	9.2500	3.3986	9.2788	11.4725	9.4845

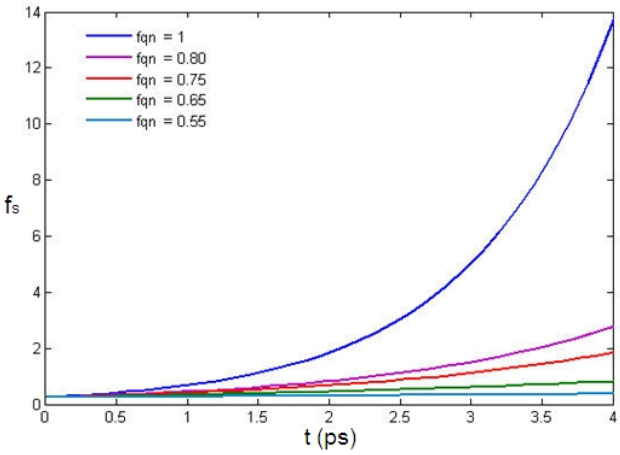

Fig. 5. Time dependency of photon levels occupancies of a QD semiconductor laser

Now, we generalize rate equation for level occupancy probabilities by spin-polarized electrons in QD and WL $(f_{w\pm}, f_{qn\pm})$ and photon spin-dependent occupancies $(f_{S\mp})$ related to QDSSPL. Thus, mathematical forms of these rate equations are [21,22]

$$\frac{df_{w\pm}}{dt} = J_{n\pm}(1-f_{w\pm}) - \frac{f_{w\pm}(1-f_{qn\pm})}{\tau_c} + \frac{2f_{qn\pm}(1-f_{w\pm})}{k\,\tau_e} \mp \frac{(f_{w+}-f_{w-})}{\tau_{snw}} \tag{4}$$

$$\frac{df_{qn\pm}}{dt} = \frac{kf_{w\pm}(1-f_{qn\pm})}{2\tau_c} - \frac{f_{qn\pm}(1-f_{w\pm})}{\tau_e} - b_q f_{qn\pm}{}^2 - g\,(2f_{qn\pm}+f_{qp\pm}-1)\,\mathrm{f}_{S\mp} + \mp\frac{(f_{qn+}-f_{qn-})}{\tau_{snq}} \tag{5}$$

$$\frac{d\ \mathrm{f}_{S\mp}}{dt} = \Gamma_{QD}\,g\,(f_{qn\pm}+f_{qp\pm}-1)\,\mathrm{f}_{S\mp} - \frac{\mathrm{f}_{S\mp}}{\tau_{ph}} \tag{6}$$

Where $J_{n\pm}$ is number of spin-polarized electrons injected into the laser per WL state and unit time. τ_{snw} and τ_{snq} are spin relaxation time in WL and QD which limit to infinite. We neglect spin-dependent spontaneous radiative recombination in WL. Note that due to charge neutrality, we could decouple the rate equations for spin-dependent electrons from those for holes. Figs. 6 and 7 determine time dependency of level occupancy probabilities by spin-up electrons in QD and WL at the fixed spin polarized injection.

These figures imply that level occupancy probabilities by spin-up electrons in WL increases by electron capture time grow up increase while level occupancy probabilities by spin-up electrons in QD increases by electron capture time reduction at the fixed spin polarized injection. As spin polarized electrons are directly injected to WL, whatever when electron capture time is shorter, spin-up electrons confine in the QDs faster and level occupancy probabilities by spin-up electrons increases in QD. Finally, as shown in Figs. 6 and 7, levels

occupancy probability by spin-up electrons in QDs and WL have constant trend and saturation is reached. Tables 4 and 5 illustrates obtained values of level occupancy probabilities by spin-up electrons in QDs and WL for three various electrons capture times.

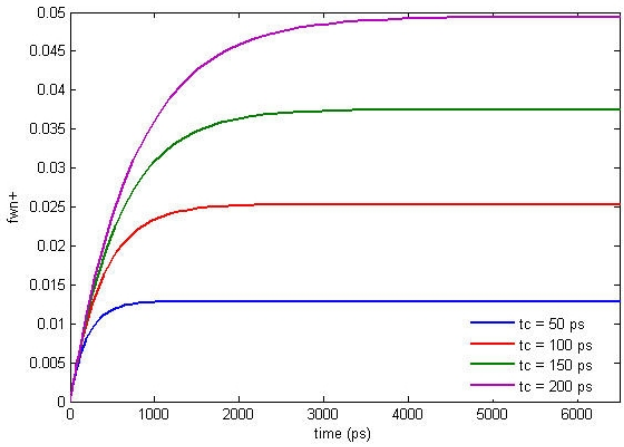

Fig. 6. Time dependency of WL levels occupancies probability by spin-up electrons for a QD SSPL

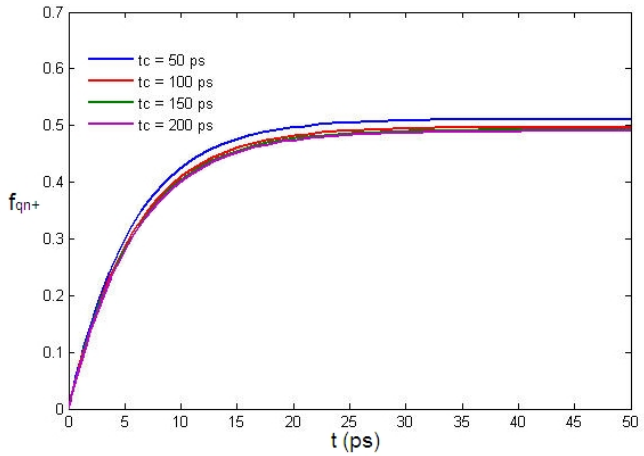

Fig. 7. Time dependency of QD levels occupancies probability by spin-up electrons for a QDSSPL

Table 4. Obtained values of levels occupancies probability by spin-up electrons in WL for three various of electron capture time

$\tau_c = 50ps$		$\tau_c = 100ps$		$\tau_c = 150ps$	
f_{w+}	$t(ps)$	f_{w+}	$t(ps)$	f_{w+}	$t(ps)$
0.0096	270.3789	0.0164	407.3349	0.0226	530.2278
0.0111	390.3743	0.0203	626.3705	0.0288	844. 1998
0.0128	1009.3	0.0253	2333.1	0.0375	3688.1

Table 5. Obtained values of levels occupancies probability by spin-up electrons in QD for three various of electron capture time

$\tau_c = 50ps$		$\tau_c = 100ps$		$\tau_c = 150ps$	
f_{qn+}	$t(ps)$	f_{qn+}	$t(ps)$	f_{qn+}	$t(ps)$
0.3500	6.4821	0.3425	6.7467	0.2736	4.7492
0.4964	19.7447	0.4823	20.1163	0.4739	18.9973
0.5099	33.4947	0.4959	33.8663	0.4917	37.7473

Fig. 8 shows time dependency of Negative Helicity (NH) photon occupancies at the fixed spin polarized injection. According to this Fig, NH photon occupancies increase with increase in levels occupancy probabilities by spin-up electrons in QD at the fixed spin-polarized injection. When level occupancy probabilities by spin-up electrons increase in QD, numbers of spin-up electrons which participate in lasing operation increase. Thus, gain increase refers to more coupling of the carriers and light. Therefore, this situation give rise to stimulated emission and lasing operation is improved.

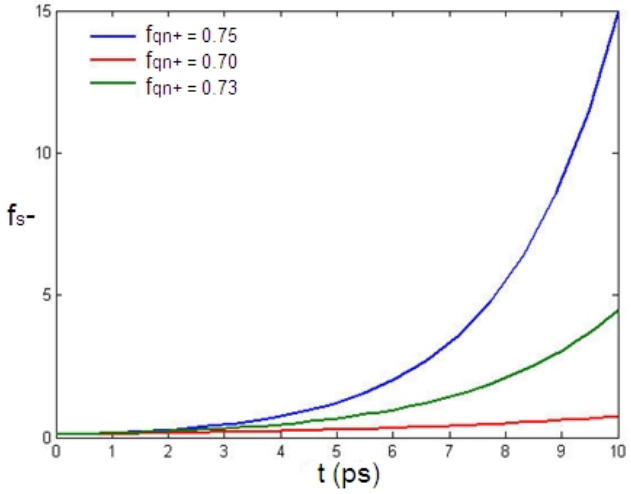

Fig. 8. Time dependency of NH photon occupancies for a QDSSPL

Table 6 shows obtained values for NH photon occupancies for three various level occupancy probabilities by spin-up electrons in QD.

Table 6. Obtained values of NH photon occupancies for three various levels occupancies probability by spin-up electrons in QD

$f_{qn+} = o.70$		$f_{qn+} = o.73$		$f_{qn+} = o.75$	
f_{s^-}	$t(ps)$	f_{s^-}	$t(ps)$	f_{s^-}	$t(ps)$
0.1051	0.2500	0.1105	0.2644	0.1163	0.3014
0.1568	2.2500	0.2377	2.2788	0.3869	2.7059
0.2858	5.2500	0.7433	5.2788	1.5283	5.4534

4. NSFI WIDTH

Creation of NSFI is one of the important consequences of spin polarized injection. The width of this interval can be obtained analytically from rate equations (4)-(6) *as* [21,22].

$$d = \left[\frac{1}{(1-|P_{Jn}|)}\right] - \left[\frac{4}{(2+|P_{Jn}|)^2} \times \left[1 + \frac{18|P^3_{Jn}|b_q\tau_c}{1+6|P_{Jn}|+3|P^2_{Jn}|-10|P^3_{Jn}|}\right]\right] \quad (7)$$

where $|P_{Jn}|$ is the polarization of injected electron current. Fig. 9 shows NSFI versus simultaneous variations of polarization of injected electron current and electron capture time.

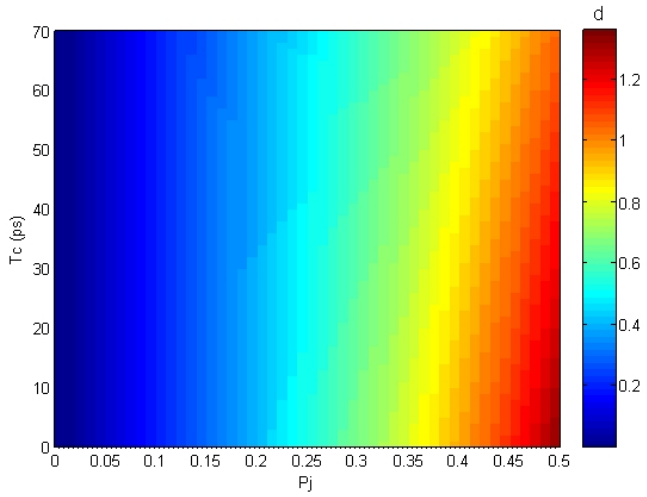

Fig. 9. NSFI versus variations of polarization of injected electron current and electron capture time

In Fig. 9 dark, red and blue areas demonstrate highest and lowest NSFI, respectively. According to it, we find out that NSFI increases with simultaneous electron capture time reduction and increase of injected electron current polarization. Increase of NSFI leads to power consumption reduction of lasers and enhances laser dynamic performance. This advantage is obtained by using electrical spin injection in QD/QW SSPLs. Fig. 10 presents NSFI versus variations of injected electron current polarization for four various electrons capture time.

Fig. 10 shows that NSFI increases with injected electron current polarization increase per specific electron capture time. When electron capture time increase, it takes a longer time for electrons to fall into QD. Thus, we observe smaller level occupancy probabilities by spin-up electrons in QD and therefore NSFI reduction. Note that up to $|P_J| = 0.12$, NSFI is equal per all electron capture time. Table 7 illustrates obtained values for NSFI for three various polarizations of injected electron current at different periods of time.

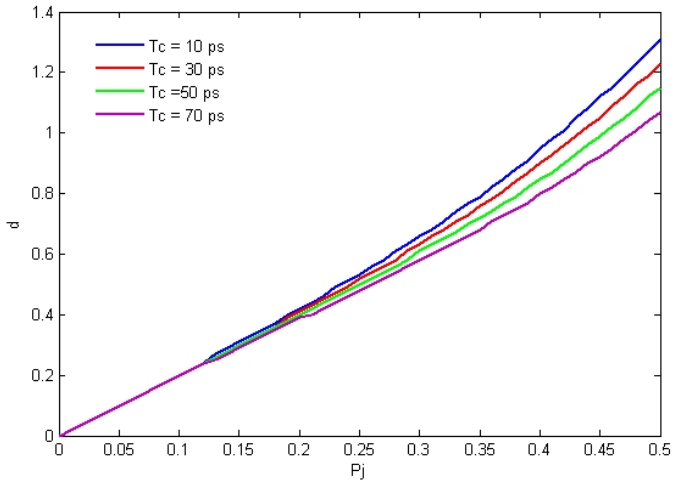

Fig. 10. NSFI versus variations of injected electron current polarization for four various electron capture times

Table 7. Obtained values of NSFI for three various polarizations of injected electron current at different period of time

$\lvert P_{Jn}\rvert = 0.2$		$\lvert P_{Jn}\rvert = 0.3$		$\lvert P_{Jn}\rvert = 0.4$	
d	$t_c(ps)$	d	$t_c(ps)$	d	$t_c(ps)$
0.41	30	0.63	30	0.90	30
0.40	50	0.61	50	0.85	50
0.39	70	0.58	70	0.80	70

From the values obtained in Table 7, we find that the NSFI maximum value is 0.90.

5. TCDR

One of the spin polarized injection benefits is TCDR which results from the creation of NSFI [23-25]. In this interval, only charge carriers with majority spin species contribute during lasing process. TCDR can be obtained analytically from rate equations (4-6) given *by the* following equation [21,22]:

$$r = 1 - \frac{4}{(2+|P_{Jn}|)^2} \times \left[1 + \frac{18|P^3{}_{Jn}|b_q \tau_c}{1+6|P_{Jn}|+3|P^2{}_{Jn}|-10|P^3{}_{Jn}|} \right] \quad (8)$$

Fig. 11 shows TCDR versus simultaneous variations of polarization of injected electron current and electron capture time.

According to Fig. 11, we find out that TCDR increases with simultaneous electron capture time reduction and increase in injected electron current polarization. Also, increase of TCDR leads to power consumption reduction of lasers and enhances laser dynamic performance. Such a reduction is obtained by using electrical spin injection in QW SSPLs. Increase of electrical spin injection leads to increase in polarization of injected electron current and laser

bandwidth. Note that TCDR increases as injected electron current polarization increases per specific electron capture time. When electron capture time increases, we observe smaller NSFI and TCDR. Table 8 illustrates obtained values for TCDR for three various polarizations of injected electron current at different period of time.

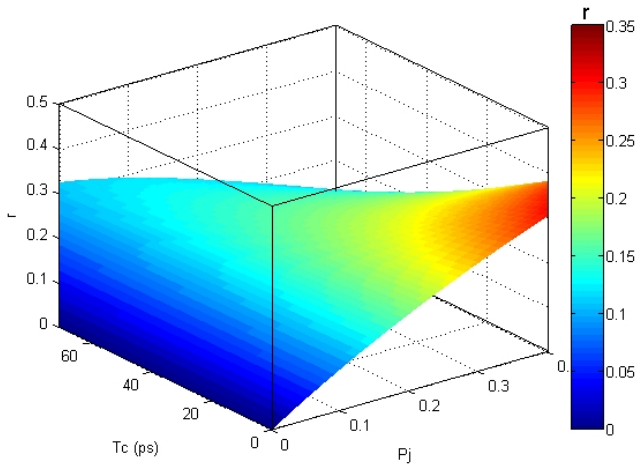

Fig. 11. TCDR versus variations of polarization of injected electron current and electron capture time

Table 8. Obtained values of TCDR for three various polarizations of injected electron current at different period of time

$\lvert P_{Jn}\rvert = 0.1$		$\lvert P_{Jn}\rvert = 0.2$		$\lvert P_{Jn}\rvert = 0.4$	
r	$t_c(ps)$	r	$t_c(ps)$	r	$t_c(ps)$
0.089	30	0.174	30	0.353	30
0.087	50	0.168	50	0.341	50
0.085	70	0.163	70	0.328	70

The values obtained in Table 8 shows the TCDR maximum at 0.353.

6. OPTICAL GAIN

The optical gain describes coupling of the carriers and light, which gives rise to stimulated emission [22,25]. According to the importance of this quantity, we intend to investigate variation of spin-dependent optical gain versus level occupancy probabilities by spin-up electrons in QD and NH photon occupancies. Spin-dependent gain term can be written as [21,22].

$$G_{\pm} = g\,(f_{qn\pm} + f_{qp\pm} - 1)\,\mathrm{f}_{S\mp} \tag{9}$$

Fig. 12 shows that spin-up gain term increases with simultaneous rising of levels occupancies probability by spin-up electrons in QD and NH photon occupancies.

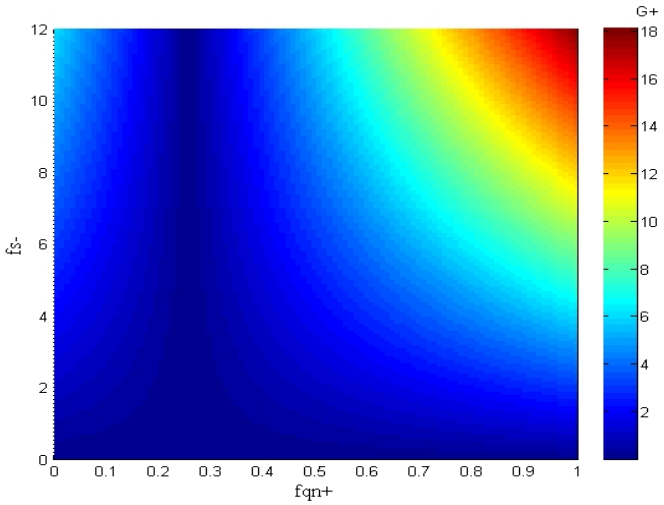

Fig. 12. Spin-up optical gain versus variations of levels occupancies probability by spin-up electrons in QD and NH photon occupancies

High level occupancy probabilities by spin-up electrons in QD lead to high NH photon occupancies, and then we obtain higher spin-up optical gain values. Increase of spin-up optical gain ensures efficiency of laser. Table 9 presents obtained values for spin-up optical gain for four various levels occupancies probability by spin-up electrons in QD.

Table 9. Obtained values of spin-up optical gain for four various level occupancy probabilities by electrons in Quantum Dots (QDs)

$f_{qn+}=1$		$f_{qn+}=0.80$		$f_{qn+}=o.75$		$f_{qn+}=0.55$	
f_{s^-}	G_+	f_{s^-}	G_+	f_{s^-}	G_+	f_{s^-}	G_+
3.5	5.40	3.5	3.96	3.5	3.60	3.5	2.16
8.2	12.45	8.2	9.13	8.2	8.30	8.2	4.98
11.7	17.70	11.7	12.98	11.7	11.80	11.7	7.08

The values obtained in Table 9 show that the spin-up optical gain maximum is obtained at 17.70.

7. CONCLUSION

According to the above discussion, there appears an intensive dependency of QD SSPL operations on spin injection and longer spin relaxation time. Using numerical rate equations, we demonstrate for the first time, the simultaneous effect of electron capture time and injected current polarization on TCDR and NSFI. It is then found that, the TCDR and NSFI increase by simultaneous electron capture time reduction and increase of injected current polarization. This increase in TCDR and NSFI leads to lower power consumption and enhances the lasers dynamic performance. The maximum values obtained for TCDR and NSFI are 0.353 and 0.90, respectively. Spin-up optical gain term increases with simultaneous rise of level occupancy probabilities by spin-up electrons in QD and NH photon occupancies. The maximum obtained Spin-up optical gain is 17.70. These results show that

laser is a very promising candidate as emerging field based on colloidal semiconductor QDs typically II–VI, such as CdS, CdSe, ZnSe, and ZnTe [26,27,28]. By providing practical paths to new spin-based devices, we expect that studies of spin-lasers will also offer motivation to understanding of spin transport and magnetism.

COMPETING INTERESTS

Authors have declared that no competing interests exist.

REFERENCES

1. Chuang SL. Physics of optoelectronic devices. 2nd ed. Wiley, New York; 2009.
2. Parker MA. Physics of optoelectronics. CRC, New York; 2004.
3. Coldren LA, Corzine SW. Diode lasers and photonic integrated circuits. (Wiley, New York; 1995.
4. Chow WW, Koch SW. Semiconductor laser fundamentals. Physics of the Gain Materials Springer, New York; 1999.
5. Haken H. Light, Vol. 2 Laser Light Dynamics North-Holland, New York; 1985.
6. Alferov ZI. Rev Mod Phys. 2001;73:767.
7. Ustinov VM, Zhukov AE, Yu A. Egorov, Maleev NA. Quantum dot lasers (Oxford University Press, New York; 2003.
8. Bimberg D, Grundmann M, Ledentsov NN. Quanutm dot heterostructures. Wiley, New York; 1999.
9. Das A, Heo J, Jankowski M, Guo W, Zhang L, Deng H, Bhattacharya P. Phys Rev Lett. 2011;107:066-405.
10. Rudolph J, H¨agele D, Gibbs HM, Khitrova G, Oestreich M, Appl Phys Lett. 2003;82:4516.
11. Rudolph J, D¨ohrmann S, H¨agele D, Oestreich M, Stolz W. Appl Phys Lett. 2005;87:2411-17.
12. Holub M, Shin J, Bhattacharya P. Phys Rev Lett. 2007;98:146-603.
13. Iba S, Koh S, Ikeda K, Kawaguchi H. Room temperature circularly polarized lasing in an optically spin injected vertical-cavity surface-emitting laser with (110) GaAs quantum wells. Appl Phys Lett. 2011;98:081-113.
14. Oestreich M, Rudolph J, Winkler R, Hagele D. Design considerations for semiconductor spin lasers. Superlattices Microstruct. 2005;37:306–312.
15. Gothgen C, Oszwałdowski R, Petrou A, Žutić I. Analytical model of spin-polarized semiconductor lasers. Appl Phys Lett. 2008;93:042-513.
16. Lee J, Falls W, Oszwałdowski R, Žutić I. Spin modulation in semiconductor lasers. Appl Phys Lett. 2010;97:0411-16.
17. Schmidt G, Ferrand D, Molenkamp LW, Filip AT, Van Wees BJ. Fundamental obstacle for electrical spin injection from a ferromagnetic metal into a diffusive semiconductor. Phys Rev. 2000;62:47-90.
18. Rashba EI. Theory of electrical spin injection: Tunnel contacts as a solution of the conductivity mismatch problem. Phys Rev. 2000;62:162-67.
19. De Groot RA, Mueller FM, Engen PGV, Buschow KHJ. New class of materials: Half-metallic ferromagnets. Phys Rev Lett. 1983;50:2024.
20. George AP. How to simulate a semiconductor quantum dot laser: General description. Brazilian Journal of Physics Teaching. 2009;31:2302.
21. Lee J, Oszwałdowski R, Gøthgen C, Žutić I. Mapping between quantum dot and quantum well lasers: From conventional to spin lasers. Phys Rev. 2012;85:045-314.

22. Oszwałdowski R, Gøthgen C, Žutić I. Theory of quantum dot spin-lasers. Phys Rev. 2010;82:085-316.
23. Rudolph J, Hägele D, Gibbs HM, Khitrova G, Oestreich M. Laser threshold reduction in a spintronic device. Appl Phys Lett. 2003;82:4516–4518.
24. Holub M, Shin J, Bhattacharya P. Electrical spin injection and threshold reduction in a semiconductor laser. Phys Rev Lett. 2007;98:146-603.
25. Basu D, Saha D, Bhattacharya P. Optical polarization modulation and gain anisotropy in an electrically injected spin laser. Phys Rev Lett. 2009;102:093-904.
26. Klimov VI. Spectral and dynamical properties of multiexcitons in semiconductor nanocrystals. Ann Rev Phys Chem. 2007;58:635.
27. Scholes GD. Controlling the optical properties of inorganic nanoparticles. Adv Funct Mater. 2008;18:1157–1172.
28. Tsymbal EEY, Žutić I. Handbook of Spin Transport and Magnetism. CRC Press. 2012;731-745.

Peer-review history:
The peer review history for this paper can be accessed here:
http://www.sciencedomain.org/review-history.php?iid=564&id=33&aid=4946